Comparison of the Accurate Kohn−Sham Solution with the Generalized Gradient Approximations (GGAs) for the S_N2 Reaction $F^- + CH_3F \rightarrow FCH_3 + F^-$: A Qualitative Rule To Predict Success or Failure of GGAs

O. V. Gritsenko, B. Ensing, P. R. T. Schipper, and E. J. Baerends*

Scheikundig Laboratorium der Vrije Universiteit, De Boelelaan 1083, 1081 HV Amsterdam, The Netherlands

Received: March 20, 2000; In Final Form: July 5, 2000

Kohn−Sham solutions are constructed from ab initio densities obtained with multireference configuration interaction (MRCI) calculations for the transition state (TS) and for the intermediate complex (IC) of the prototype symmetrical S_N2 reaction $F^- + CH_3F \rightarrow FCH_3 + F^-$. The calculated KS exchange and correlation energies, E_x^{KS} and E_c^{KS}, as well as the exchange and exchange-correlation (xc) energy densities $\epsilon_x^{KS}(\mathbf{r})$ and $\epsilon_{xc}^{KS}(\mathbf{r})$, are compared with the corresponding quantities of the standard generalized gradient approximation (GGA). GGA functionals substantially underestimate the repulsive exchange contribution to the central barrier of the S_N2 reaction, thus producing a too low barrier. A similar problem arises in a number of other bonding situations, and a qualitative rule is put forward to predict success or failure of standard GGAs in molecular calculations, depending on the type of chemical bonding. For systems with two-center two-electron bonds (standard covalent bonds), two-center four-electron Pauli repulsion (interacting closed shells), and three-center three-electron bonds, current GGAs (or minor modifications) are expected to perform successfully. In these cases the GGA exchange functional represents exchange and (if it is present) nondynamical Coulomb correlation, while the GGA correlation functional represents dynamical Coulomb correlation. Contrary to this, for systems with three-center four-electron bonds (TS of the S_N2 reaction), two-center three-electron bonds, and two-center one-electron bonds, for which the exchange hole is delocalized over all interacting fragments and efficient nondynamical correlation is hampered by the unfavorable electron count, the GGA exchange functionals still yield nondynamical correlation, which is in these cases spurious, the GGAs thus overestimating the relative stability of these systems.

I. Introduction

Methods of density functional theory (DFT),[1] especially the generalized gradient approximations (GGAs),[2−5] have become a standard tool for theoretical study of chemical bonding and molecular reactions. However, some reactions and types of bonding appear to be problematic cases for DFT applications. In particular, standard approximate DFT methods systematically overestimate dissociation energies of two-center three-electron bonds[6−8] and they underestimate barriers of radical abstraction reactions[9−17] and of bimolecular nucleophilic substitution (S_N2) reactions.[18−20]

A promising way to analyze systematically the performance of DFT methods is to compare their results with the essentially accurate Kohn−Sham (KS) solution, which can be obtained from an accurate ab initio electron density $\rho(\mathbf{r})$. Previously, such solutions have been obtained for a number of atoms[21−24] and molecules.[25−32] In ref 17, the accurate KS solutions have been compared with GGAs for the simplest prototype reactions $H + H_2$ and $H_2 + H_2$.

In this paper, the Kohn−Sham solution is constructed from ab initio densities obtained with multireference configuration interaction (MRCI) calculations for the transition state (TS) and for the intermediate complex (IC) of the prototype symmetrical S_N2 reaction

$$F^- + CH_3F \rightarrow FCH_3 + F^- \qquad (1.1)$$

Bimolecular nucleophilic substitution reactions at tetrahedral carbon centers represent one of the most basic of chemical transformations. Reactions $X^- + CH_3X \rightarrow XCH_3 + X^-$, where X is a halide atom, occur in the gas phase[33−35] and for the prototype reaction 1.1 with the lightest halide atom F, high-quality ab initio calculations have been performed with the coupled-cluster CCSD(T)[36] and G2(+)[37] methods. As was established in ref 18, standard DFT methods, such as the local density approximation (LDA) and a combination (BP) of the GGA exchange energy functional (B88) of Becke[4] and GGA correlation functional (P86) of Perdew,[2] consistently underestimate barriers of the reactions $X^- + CH_3X \rightarrow CH_3 + X^-$.

In section II of this paper, the results of ab initio MRCI calculations of the reaction 1.1 are presented. With reference configurations which reproduce the proper dissociation limit of the three-center bond F−C−F, and with the correlation-consistent triple-ζ basis, MRCI is capable of describing correctly the relative stability of the TS and IC of (1.1). In section III the KS solution is constructed from the ab initio density ρ, and the KS exchange E_x^{KS} and correlation E_c^{KS} energies as well as the exchange $\epsilon_x^{KS}(\mathbf{r})$ and exchange-correlation (xc) $\epsilon_{xc}^{KS}(\mathbf{r})$ energy densities are obtained for the TS and IC. A substantially less negative E_x^{KS} when going from IC to TS indicates relative delocalization of the exchange hole for valence electrons over all three fragments of the TS $[F\cdots CH_3\cdots F]^-$. This less negative value of E_x^{KS} is not compensated by the slightly more negative value of E_c^{KS}, so that the KS xc energy E_{xc}^{KS} becomes smaller (less negative) in the TS. Calculations in the same basis with standard GGA methods, which are based on localized model exchange and correlation holes, fail to describe the smaller

10.1021/jp001061m CCC: $19.00
Published on Web 08/24/2000

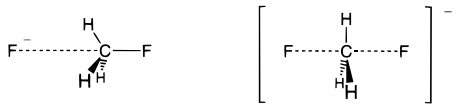

Figure 1. Schematic representation of ion−dipole intermediate complex (IC) and the transition state (TS).

exchange-correlation energy corresponding to the delocalized hole, thus overestimating the relative stability of the TS.

A qualitative rule is put forward in section IV to predict the success or failure of GGAs for a chemical bond, which involves *m* fragment orbitals and *n* electrons. Current GGAs, or minor modifications, are expected to perform better in cases when the ratio *n/m* is an integer number. These are the cases of standard covalent bonds with 2 fragment orbitals and 2 electrons per bond ($n/m = 1$, with N_2 as an example) or 2 orbitals and 4 electrons ($n/m = 2$, interacting closed shells) as well as the case of 3 orbitals and 3 electrons ($n/m = 1$, TS of the hydrogen abstraction reaction $H + H_2$). In these cases the GGA exchange functional is expected to represent properly both exchange and nondynamical left−right correlations which, taken together, produce a localized XC hole. However, GGAs might fail in the cases where the ratio *n/m* is a fractional number. These are the cases of 2 orbitals and 1 electron ($n/m = 1/2$, H_2^+), 2 orbitals and 3 electrons ($n/m = 3/2$, F_2^- or $(H_2O)_2^+$), and 3 orbitals and 4 electrons ($n/m = 4/3$, TS of the S_N2 reaction $F^- + CH_3F$), in which the exchange hole for valence electrons is delocalized, while nondynamical correlation is absent or hampered due to an unfavorable electron count. In these cases, standard GGAs are expected to consistently overestimate the stability of corresponding structures. In section V, possible ways to overcome this failure of GGAs are discussed and the conclusions are drawn.

II. MRCI Calculations of the S_N2 Reaction

Two characteristic intermediates in the S_N2 reaction 1.1 are the ion−dipole intermediate complex (IC) $F^-\cdots CH_3F$ and the symmetrical transition state (TS) $[F\cdots CH_3\cdots F]^-$, which are schematically shown in Figure 1. The ab initio calculations of TS, IC, and the isolated reactants have been performed in this paper with the multireference configuration interaction (MRCI) method by means of the ATMOL package.[38] Within MRCI, all single and double excitations of a number of reference configurations are taken into account in a given basis. The actual geometry has been taken from ref 36 where it was optimized with high quality coupled-cluster CCSD(T) calculations.

To analyze the basis set effect, two triple-ζ (TZ) quality basis sets (B1) and (B2) have been employed for the heavier elements C and F. B1 is the (6s4p1d) basis of ref 36 which has been obtained by addition of polarization functions to the (5s3p) basis of ref 39 B2 is the (4s3p2d) basis of the same size as B1, which has been obtained from the correlation-consistent polarized valence TZ (cc-pVTZ) basis (4s3p2d1f) of ref 40 by means of removal of its *f*-function. For the H atom the (4s1p) basis of ref 36 has been used, which is the (3s) basis of ref 39 augmented with polarization functions. Thus, the total basis sets for the system $CH_3F_2^-$ based either on B1 or on B2 both contain 90 contracted Gaussian functions. Three reference configurations have been used for the MRCI, which reproduce the proper limit of dissociation of the three-center bond F−C−F in the TS.

One of the key characteristics of S_N2 reactions is the central reaction barrier E^b, which is the difference of the total energies of TS and IC, $E^b = E(TS) - E(IC)$. Table 1 presents E^b obtained with the Hartree−Fock (HF), single-reference CI (SRCI), and MRCI calculations in the basis sets B1 and B2. They are compared with E^b of the benchmark CCSD(T) calculations of ref 36 which were performed in the same basis B1, while B2 in this case is the quadruple-ζ basis constructed in ref 36 from the (5s4p) basis of ref 39. One can see from Table 1 that both basis quality and quality of the method employed are important, in order to get a good estimate of the barrier height. The correlation-consistent basis B2, which was optimized in ref 40 with atomic CI calculations, yields lower total energies of both TS and IC than B1, and both SRCI and MRCI E^b values obtained with B2 are closer to the B2-CCSD(T) value than the respective B1-SRCI and B1-MRCI barriers. Note that HF/CI calculations show stronger dependence on basis than the coupled-cluster calculations of ref 36. The Hartree−Fock (HF) method tends to overestimate the barrier; the corresponding errors with respect to CCSD(T) are 5.9 kcal/mol in the basis B1 and 4.3 kcal/mol in B2. SRCI partially corrects this error and our SRCI value is very close to $E^b = 17.1$ kcal/mol of the earlier CI calculations.[41] MRCI produces further improvement and the value $E^b = 13.69$ kcal/mol obtained with MRCI in the basis B2 is only 0.3 kcal/mol higher than the benchmark CCSD(T) value $E^b = 13.41$ kcal/mol.

TABLE 1: Central Barriers $E^b = E(TS) - E(IC)$ (kcal/mol) for $[F^-\cdots CH_3F] \rightarrow FCH_3F]^-$ Calculated with ab Initio Methods

basis	HF	SRCI	MRCI	CCSD(T)[a]
B1	19.22	17.05	15.42	13.29
B2	17.72	15.20	13.69	13.41

[a] Reference 36. In the CCSD(T) calculations basis B1 is exactly the same, and basis B2 contains an additional *f* function compared to the HF and CI calculations.

On the other hand, the present CI calculations substantially underestimate stability of IC and TS with respect to the reagents CH_3F and F^-. In particular, the total energy of IC obtained with our best CI calculation (MRCI and B2) is still 0.2 kcal/mol higher than the sum of the total energies of individual reactants CH_3F and F^- calculated with SRCI and B2. However, according to the CCSD(T) calculations of ref 36, $CH_3F\cdots F^-$ is a stable complex with an energy of complexation $\Delta E(IC) = -13.17$ kcal/mol. This error can be attributed to the size inconsistency[42] of the restricted CI, because of which it recovers a larger portion of the electron correlation for smaller fragments than for the corresponding compound system. Note that the HF method, which does not suffer from the size-inconsistency error, yields a good estimate $\Delta E(IC) = -11.64$ kcal/mol in the basis B2 of ref 36.

Still, the results of this section confirm the expectation that, given proper reference configurations and basis set, MRCI is capable of describing correctly the relative stability of molecular structures of similar size. In particular, the present MRCI calculations with three reference configurations and with the correlation-consistent triple-ζ basis describe very well the relative stability of TS and IC of the S_N2 reaction 1.1. In the next section, the MRCI electron density ρ will be used to construct relatively accurate KS solutions for TS and IC.

III. KS Solution and GGA Calculations for the S_N2 Reaction

The Kohn−Sham orbitals $\psi_i(\mathbf{r})$ and potential $v_s(\mathbf{r})$ for TS and IC of the S_N2 reaction 1.1 have been obtained from the MRCI density $\rho(\mathbf{r})$ with the iterative procedure of ref 43, which is based on the theory of linear response of the KS orbitals to a potential change δv_s. Using these $\{\psi_i(\mathbf{r})\}$, the KS kinetic

TABLE 2: Contributions (kcal/mol) of the KS and GGA Exchange and Correlation Functionals to the Central Barrier (Energy of Transition State Minus Intermediate Complex) $[F^-\cdots CH_3F] \rightarrow FCH_3F]^-$

	PW	BP	BLYP	KS
E_x^b	12.96	13.58	13.58	28.87
E_c^b	0.38	−0.05	−0.82	−3.19
E_{xc}^b	13.34	13.53	12.76	25.68

energy T_s

$$T_s = \sum_{i=1}^{N} \int d\mathbf{r} \psi_i^*(\mathbf{r})(-{}^1/_2\nabla^2)\psi_i(\mathbf{r}) \tag{3.1}$$

and the exchange energy E_x^{KS}

$$E_x^{KS} = -\frac{1}{4}\sum_{i=1}^{N}\sum_{j=1}^{N} \int d\mathbf{r}_1\, d\mathbf{r}_2 \frac{\psi_i^*(\mathbf{r}_1)\psi_j(\mathbf{r}_1)\psi_j^*(\mathbf{r}_2)\psi_i(\mathbf{r}_2)}{|\mathbf{r}_1 - \mathbf{r}_2|} \tag{3.2}$$

have been calculated, and the KS correlation energy E_c^{KS} can been obtained from the MRCI or CCSD(T) total electronic energy E^{MRCI} or $E^{CCSD(T)}$ from the following expression

$$E_c^{KS} = E^{MRCI} - T_s - \int d\mathbf{r}\, \rho(\mathbf{r}) v_{ext}(\mathbf{r}) - \frac{1}{2}\int d\mathbf{r}_1\, d\mathbf{r}_2 \frac{\rho(\mathbf{r}_1)\rho(\mathbf{r}_2)}{|\mathbf{r}_1 - \mathbf{r}_2|} - E_x^{KS} \tag{3.3}$$

The absolute value of E_c^{KS} suffers from the size-consistency error in the MRCI calculations that we noted earlier, but we will only use differences in E_c^{KS} between TS and IC, so that the errors cancel and it is immaterial whether we use E^{MRCI} or $E^{CCSD(T)}$ in eq 3.3.

The key quantities for our analysis are the exchange and correlation contributions, E_x^b and E_c^b, to the central reaction barrier E^b, which are the differences of the corresponding energies of TS and IC, $E_x^b = E_x^{KS}(TS) - E_x^{KS}(IC)$ and $E_c^b = E_c^{KS}(TS) - E_c^{KS}(IC)$. They are presented in the last column of Table 2. The exchange brings a large positive contribution $E_x^b = 28.9$ kcal/mol to E^b. This can be understood from the exchange (Fermi) hole function $\rho_x(\mathbf{r}_2|\mathbf{r}_1)$, which gives the exchange energy E_x^{KS}

$$E_x^{KS} = \frac{1}{2}\int \frac{\rho(\mathbf{r}_1)\rho_x(\mathbf{r}_2|\mathbf{r}_1)}{|\mathbf{r}_1 - \mathbf{r}_2|} d\mathbf{r}_1 d\mathbf{r}_2 \tag{3.4}$$

and which can be defined from (3.2) and (3.4) as follows

$$\rho_x(\mathbf{r}_2|\mathbf{r}_1) = -\frac{1}{2\rho(\mathbf{r}_1)}\sum_{i=1}^{N}\sum_{j=1}^{N} \frac{\psi_i^*(\mathbf{r}_1)\psi_j(\mathbf{r}_1)\psi_j^*(\mathbf{r}_2)\psi_i(\mathbf{r}_2)}{|\mathbf{r}_1 - \mathbf{r}_2|} \tag{3.5}$$

For IC the exchange in individual fragments F^- and CH_3F derives from an exchange hole which is localized within the fragment where the reference electron is located. This can easily be understood from the fact that the exchange hole has approximately the shape of the localized orbital with large amplitude at the reference position.[44,45] Formation of the three-center bond F···C···F in the TS causes delocalization of the exchange hole in the bonding region over all fragments (orbital localization will be less effective than in the IC). The delocalization of the exchange hole charge of one electron produces a decrease of the exchange energy (it becomes less negative), and hence the observed positive contribution E_x^b to the barrier. The correlation contribution to the barrier $E_c^b = -3.2$ kcal/mol is on the contrary negative and small, so that the combined xc contribution to the barrier E_{xc}^b is positive and close to E_x^b (see Table 2). Note that E_c^b of the KS theory is close to the correlation contribution $E_c^b(\text{MRCI-HF}) = E^{b(MRCI)} - E^{b(HF)} = -4$ kcal/mol calculated according to the conventional quantum chemical definition of correlation energy from the MRCI and HF barrier heights of Table 1.

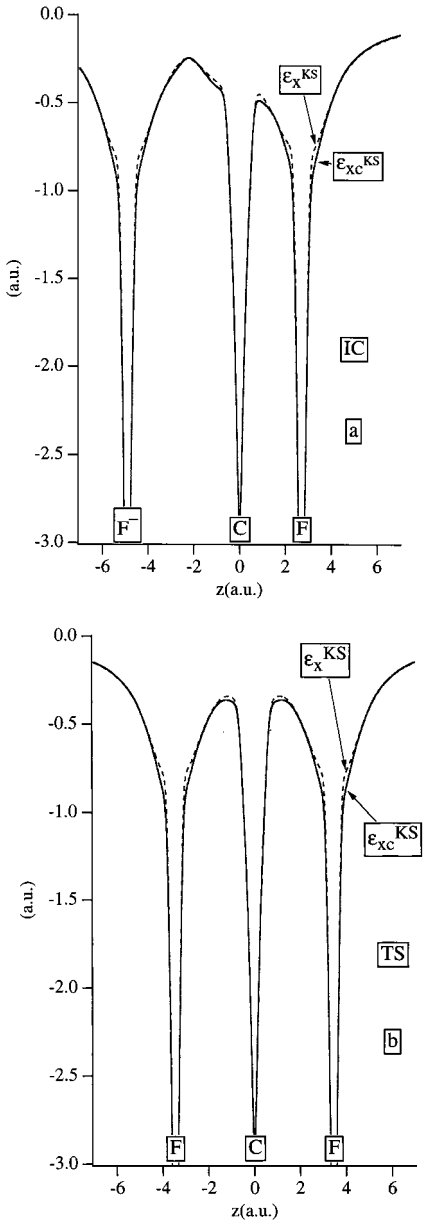

Figure 2. Comparison of the Kohn−Sham exchange and exchange-correlation energy densities (z is the F−C−F bond axis): (a) ion−dipole intermediate complex (IC) and (b) transition state (TS).

Figure 2 compares the KS exchange and xc energy densities, $\epsilon_x^{KS}(\mathbf{r})$ and $\epsilon_{xc}^{KS}(\mathbf{r})$, constructed according to the definitions given in refs 27, 46, and 47, for the TS and the IC along the bond F···C···F. The energy densities yield the corresponding exchange and xc energies

$$E_x^{KS}[\rho] = \int \rho(\mathbf{r}) \epsilon_x^{KS}([\rho];\mathbf{r})\, d\mathbf{r} \tag{3.6}$$

$$E_{xc}^{KS}[\rho] = \int \rho(\mathbf{r}) \epsilon_{xc}^{KS}([\rho];\mathbf{r})\, d\mathbf{r} \tag{3.7}$$

and they have been constructed from the MRCI wave function

TABLE 3: Comparison of the GGA and ab Initio Central Barriers (kcal/mol) for $[F^-\cdots CH_3F] \rightarrow FCH_3F]^-$[a]

	PW	BP	BLYP	MRCI	CCSD(T)[b]
"exact"				13.69	13.41
KS/GGA	1.35	1.54	0.77		
full GGA	1.52	1.99	1.78		

[a] The row labeled "full GGA" is based on energies from standard SCF GGA calculations, so ψ^{GGA} has been used for T_s and ρ^{GGA} for all other terms (electron−nuclear, electron−electron Coulomb terms, and E_{xc}^{GGA}). The row labeled KS/GGA uses ψ^{KS} for T_s and ρ^{MRCI} for the other terms including $E_{xc}^{GGA}[\rho^{MRCI}]$. [b] Reference 36.

by means of a Gaussian orbital density functional code[25,29,48] based on the ATMOL package. The characteristic features of $\epsilon_x^{KS}(\mathbf{r})$ and $\epsilon_{xc}^{KS}(\mathbf{r})$ are wells around the nuclei and peaks in the bond midpoint regions. The form of the total xc function $\epsilon_{xc}^{KS}(\mathbf{r})$ is determined by the dominating exchange effects: $\epsilon_{xc}^{KS}(\mathbf{r})$ is close to its exchange component $\epsilon_x^{KS}(\mathbf{r})$, and differs visibly only at the borders of the regions of core and valence electron shells, and around the bond midpoint. The form of $\epsilon_x^{KS}(\mathbf{r})$ and $\epsilon_{xc}^{KS}(\mathbf{r})$ for IC is clearly unsymmetrical with respect to two F atoms (see Figure 2a). The bond midpoint peak for the C−F bond in CH_3F is considerably lower than the peak for the bond $F^-\cdots C$, which correlates with the greater strength of the former bond. Formation of the symmetrical three-center bond $F\cdots C\cdots F$ in the TS is reflected in a symmetrical form of $\epsilon_x^{KS}(\mathbf{r})$ and $\epsilon_{xc}^{KS}(\mathbf{r})$ (see Figure 2b), and the corresponding bond midpoint peaks are higher than that for the C−F bond in IC, but they are lower than the peak of the $F^-\cdots C$ bond in IC.

The GGA functionals considered in this paper are the xc functional of Perdew and Wang (PW91),[5,49,50] the combination BP of the exchange functional of Becke (B88)[4] and the correlation functional of Perdew (P86)[2] and the combination BLYP of the same exchange functional B88 with the correlation functional of Lee, Yang, and Parr.[3] The GGA calculations have been performed both self-consistently and with the MRCI $\rho(\mathbf{r})$ in the same basis B2, which has been used for the MRCI calculation. In Table 3 the central barriers of the reaction 1.1 $E^{b(GGA)}$ calculated with GGAs are compared with the ab initio MRCI and CCSD(T) ones. The row labeled "full GGA" is based on energies from standard SCF GGA calculations, so ψ^{GGA} has been used for T_s and ρ^{GGA} for all other terms (electron−nuclear, electron−electron Coulomb terms and E_{xc}^{GGA})

$$E^{GGA} = T_s^{GGA} + \int d\mathbf{r}\, \rho^{GGA}(\mathbf{r}) v_{ext}(\mathbf{r}) + \frac{1}{2}\int d\mathbf{r}_1\, d\mathbf{r}_2 \frac{\rho^{GGA}(\mathbf{r}_1)\rho^{GGA}(\mathbf{r}_2)}{|\mathbf{r}_1 - \mathbf{r}_2|} + E_x^{GGA}[\rho^{GGA}] + E_c^{GGA}[\rho^{GGA}] \quad (3.8)$$

The row labeled KS/GGA uses ψ^{KS} for T_s and ρ^{MRCI} for the other terms including $E_{xc}^{GGA}[\rho^{MRCI}]$

$$E^{KS/GGA} = T_S + \int d\mathbf{r}\, \rho^{MRCI}(\mathbf{r}) v_{ext}(\mathbf{r}) + \frac{1}{2}\int d\mathbf{r}_1\, d\mathbf{r}_2 \frac{\rho^{MRCI}(\mathbf{r}_1)\rho^{MRCI}(\mathbf{r}_2)}{|\mathbf{r}_1 - \mathbf{r}_2|} + E_x^{GGA}[\rho^{MRCI}] + E_c^{GGA}[\rho^{MRCI}] \quad (3.9)$$

The differences in the kinetic energy, electron−nuclear, and electron−electron Coulomb energies between eqs 3.8 and 3.9 are individually not small, but their sums are much closer to each other, the corresponding differences are about 0.05 hartree. Furthermore, these differences are systematic for both TS and IC, so that they cancel each other in the calculated barrier heights. Since also the GGA exchange and correlation energies do not differ much when evaluated with ρ^{MRCI} compared to ρ^{GGA}, the full GGA and KS/GGA energies do not differ much and yield approximately the same result for the barrier heights, the largest diference being 1 kcal/mol for BLYP; see Table 3. Comparing to the accurate MRCI and CCSD(T) values for the barrier heights, we note that all GGAs greatly underestimate the barrier of the S_N2 reaction: the GGA barriers are in the range 1−2 kcal/mol, some 12−13 kcal/mol lower than the MRCI barrier of 13.7 kcal/mol or the CCSD(T) barrier of 13.4 kcal/mol.

Since the first three terms of eq 3.9 are identical to the same terms in the exact (MRCI) energy, the only possible source of error is in the exchange and correlation GGA functionals. Bearing this in mind, we compare in Table 2 the contributions $E_x^{b(GGA)}$ and $E_c^{b(GGA)}$ of the GGA exchange and correlation functionals to the barrier $E^{b(GGA)}$ with the corresponding KS contributions E_x^b and E_c^b that we already dscussed. The $E_x^{b(GGA)}$ and $E_c^{b(GGA)}$ are not very sensitive to the quality of the density used to evaluate them and would not change much when calculated with ρ^{GGA}. They are calculated with the MRCI $\rho(\mathbf{r})$, and therefore the difference in the KS E_{xc}^b and a GGA E_{xc}^b in Table 2 is precisely the same as the difference between the total MRCI barrier energy and the KS/GGA barrier in Table 3. So the source of the GGA error is in the GGA exchange-correlation functionals, in fact almost completely in the exchange part. Indeed, both B88 and PW91 exchange functionals substantially overestimate the electron exchange in the TS, yielding a too negative exchange energy in the TS and thus underestimating the repulsive contribution of the exchange to the barrier. The corresponding errors, comparing to the exact KS exchange energy, are 15.3 and 15.9 kcal/mol for B88 and PW91 exchange functionals, respectively. The GGA correlation functionals PW91, P86, and LYP produce small errors of opposite sign; i.e., they underestimate the attractive contribution of the electron correlation to the barrier (see Table 2). However, these small errors cannot compensate the errors of the exchange functionals. As a result, the total xc contribution to the barrier E_{xc}^b is substantially underestimated (12−13 kcal/mol) by the GGAs. The interpretation of this failure of GGAs for the S_N2 reaction will be given in the next section.

IV. A Qualitative Rule To Predict Success or Failure of GGAs

To rationalize the results of the present calculations of the S_N2 reaction and our previous results[17,28,29] as well as other cited literature data, we propose the following qualitative rule to predict the success or failure of GGAs for a molecule with a chemical bond, which involves *m* fragment orbitals and *n* electrons.

The success or failure of GGAs can be predicted from the ratio n/m of the number n of electrons involved in a given chemical bond, to the number m of relevant fragment orbitals.

Current GGAs, with maybe minor improvements, are expected to perform better in cases where the ratio n/m is an integer number.

GGAs might fail in cases where the ratio n/m is a fractional number.

Below we shall present the justifications of this rule and the corresponding examples.

(a) $n/m = 1$, Standard Covalent Bonds with $n = 2$ Electrons and $m = 2$ Fragment Orbitals (Example: N_2). The most common type of bonding is a standard covalent bond,

TABLE 4: Comparison of the GGA and KS Exchange and Correlation Energies (au) for the N_2 Molecule

functional	E_x	E_c	E_{xc}
PW/PW	−13.180	−0.490	−13.670
BPW	−13.208	−0.490	−13.698
BLYP	−13.208	−0.484	−13.692
KS	−13.114	−0.552	−13.666
	$E_x^{KS} + E_c^{nd}$	$E_c^{KS} - E_c^{nd}$	
	−13.190	−0.476	

which involves $n = 2$ electrons and $m = 2$ orbitals $a(\mathbf{r})$ and $b(\mathbf{r})$ of interacting fragments A and B. In this case the exchange hole $\rho_x(\mathbf{r}_2|\mathbf{r}_1)$ in the bonding region has the shape of the bonding MO $\psi_+(\mathbf{r}) = N_+[a(\mathbf{r}) + b(\mathbf{r})]$, so that it is delocalized over both fragments irrespective of the reference position $\mathbf{r}_1$. A typical covalent bond is also characterized by a relatively strong nondynamical left−right Coulomb correlation, which becomes particularly strong in long-distance/weak bonding situations. Within the CI it is described by the interaction of the main configuration, with $\psi_+(\mathbf{r})$ doubly occupied, with the doubly excited configuration, with the fully occupied antibonding MO $\psi_-(\mathbf{r}) = N_-[a(\mathbf{r}) - b(\mathbf{r})]$. The corresponding correlation hole function $\rho_c(\mathbf{r}_2|\mathbf{r}_1)$, which defines the potential part of the correlation energy W_c

$$W_c = \frac{1}{2}\int \frac{\rho(\mathbf{r}_1)\rho_c(\mathbf{r}_2|\mathbf{r}_1)}{|\mathbf{r}_1 - \mathbf{r}_2|} d\mathbf{r}_1\, d\mathbf{r}_2 \qquad (4.1)$$

is also delocalized over both fragments A and B. If the reference position $\mathbf{r}_1$ is on fragment A, $\rho_x(\mathbf{r}_2|\mathbf{r}_1)$ and $\rho_c(\mathbf{r}_2|\mathbf{r}_1)$ have opposite sign on B and cancel each other there, while on A they are both negative and build together a localized xc hole at A around $\mathbf{r}_1$. (We refer to ref 45 for an extensive discussion of the shape and behavior of exchange and correlation holes.)

This bonding situation is favorable for GGAs, which are based on models with localized exchange and correlation holes. The N_2 molecule with a single σ and two π bonds provides an example of covalent bonding. Each bond of N_2 involves two fragment σ- or π-orbitals ($m = 2$) and two electrons ($n = 2$). The KS solution for N_2 has been constructed and compared with GGAs in refs 28 and 29, and Table 4 presents the KS and GGA exchange and correlation energies calculated at the equilibrium N−N distance (in all calculations the same MRCI density $\rho(\mathbf{r})$ has been used). The last row of Table 4 presents the sum ($E_x^{KS} + E_c^{nd}$) of the KS exchange energy E_x^{KS} and the energy of nondynamical correlation E_c^{nd} as well as the difference ($E_c^{KS} - E_c^{nd}$) between the KS correlation energy E_c^{KS} and E_c^{nd}. The energy E_c^{nd} has been estimated as the difference $E_c^{nd} = E^{PDL} - E^{HF}$ between the electronic energy E^{PDL} of a simple CI wave function, which provides the proper dissociation limit (PDL),[51] and the HF electronic energy E^{HF}.

As one can see from Table 4, the GGA energies E_x^B and E_x^{PW} are substantially more negative than the KS exchange energy E_x^{KS}. Since the self-interaction correction (SIC) term

$$E_x^{KS(SIC)} = -\frac{1}{2}\sum_{i=1}^{N}\int d\mathbf{r}_1\, d\mathbf{r}_2 \frac{|\psi_i(\mathbf{r}_1)|^2|\psi_i(\mathbf{r}_2)|^2}{|\mathbf{r}_1 - \mathbf{r}_2|} \qquad (4.2)$$

constitutes a major part of E_x^{KS}, this GGA error can be called a self-interaction overestimation error. However, this error brings the GGA energies E_x^B and E_x^{PW} quite close to the sum ($E_x^{KS} + E_c^{nd}$) and this is not a mere accident. Indeed, as was mentioned above, a combination of the exchange and nondynamical correlation produces in this case a localized xc hole, while GGA functionals are based on localized model holes. This means that the GGA exchange functionals represent effectively not only exchange, but also the nondynamical left−right correlation in N_2. In their turn, the GGA energies E_c^{PW} and E_c^{LYP} are substantially less negative than the KS correlation energy E_c^{KS}, but they are quite close to the difference ($E_c^{KS} - E_c^{nd}$). This means that the GGA correlation functionals represent the dynamical Coulomb correlation. As a result, the total GGA exchange-correlation energies are close to the KS E_{xc}^{KS}, which is especially true for the PW91 functional.

TABLE 5: Reaction Barriers E^b for the Reaction H + H_2 with the Exchange and Correlation Contributions (kcal/mol)[a]

	CI/KS	PW	BP	BLYP
E^b	9.64	4.2	1.6	3.8
E_x^b	29.70	18.1	18.7	18.7
E_c^b	−14.47	−8.3	−11.5	−9.3
E_{xc}^b	15.23	9.8	7.2	9.4

[a] The E_x^{GGA} and E_c^{GGA} are calculated using ρ^{MRCI}. The barrier energies in the GGA columns refer to KS/GGA energies for TS and IC, cf. Table 3. The CI/KS and KS/GGA total energies and barrier energies differ only in the exchange-correlation terms.

(b) $n/m = 2$, Interacting Closed Shells with $n = 4$ Electrons and $m = 2$ Fragment Orbitals. Pure interaction of this type is a specific feature of the noble gas dimers, such as He_2 and Ne_2, for which the KS solutions have been constructed and analyzed in ref 52. The case of $n = 4$ and $m = 2$ is just the case of He_2, for which bonding $\psi_+(\mathbf{r}) = N_+[a(\mathbf{r}) + b(\mathbf{r})]$ and antibonding $\psi_-(\mathbf{r}) = N_-[a(\mathbf{r}) - b(\mathbf{r})]$ MOs are both occupied. In this case both exchange $\rho_x(\mathbf{r}_2|\mathbf{r}_1)$ and correlation $\rho_c(\mathbf{r}_2|\mathbf{r}_1)$ holes are localized within the atom, where the reference electron is located. This situation is also favorable for GGAs and individual GGA functionals represent the effects they were designed for: the GGA exchange functional represents just the atomic exchange and the GGA correlation functional represents the atomic dynamical correlation. The dominant effect of the interaction of closed shells, the Pauli repulsion, is reproduced correctly by GGA calculations, since the major contributing energetic effects, such as rise of the kinetic energy due to the filling of antibonding orbitals, and change in the electron−nuclear potential energy due to density change caused by the antisymmetrization of the product of monomer wave functions, are represented in the KS calculations, and are not sensitive to the quality of the exchange-correlation approximation.

(c) $n/m = 1$, TS of Radical Abstraction Reactions, with a Three-Center ($m = 3$) Three-Electron ($n = 3$) Bond (example: TS of the Hydrogen Abstraction Reaction H + H_2). A three-center three-electron bond is formed in the transition state (TS) of the radical abstraction reaction. The simplest example is the hydrogen abstraction reaction H + H_2 with the symmetrical TS $H_a\cdots H_c\cdots H_b$, in which all three electrons, two orbitals of terminal H atoms $a(\mathbf{r})$, $b(\mathbf{r})$ and the orbital $c(\mathbf{r})$ of the central H atom are involved in the three-center three-electron bond H···H···H. This bond is represented with the doubly occupied bonding orbital $\psi_+(\mathbf{r}) = d_{1+}a(\mathbf{r}) + d_{2+}c(\mathbf{r}) + d_{1+}b(\mathbf{r})$ and singly occupied nonbonding orbital $\psi_0(\mathbf{r}) = d_{10}a(\mathbf{r}) - d_{10}b(\mathbf{r})$. The bond is characterized by a substantial nondynamical correlation, which is described within the CI with electron excitations to the antibonding orbital (unoccupied in the main configuration) $\psi_-(\mathbf{r}) = d_{1-}a(\mathbf{r}) - d_{2-}c(\mathbf{r}) + d_{1-}b(\mathbf{r})$ and also with excitations from and to the singly occupied orbital ψ_0.

The KS solution for the reaction H + H_2 has been constructed and compared with GGAs in ref 17. In Table 5 the MRCI reaction barrier $E°$ and the KS exchange and correlation contributions to the barrier are compared with the corresponding

GGA values. As in the case of the S_N2 reaction, the KS exchange contribution $E_x^{b(KS)} = 29.7$ kcal/mol to the barrier is relatively large and positve. However, unlike the S_N2 case, the increased nondynamical correlation in the H···H···H transition state brings a substantial negative contribution to the barrier (a relatively large negative value of $E_c^{b(KS)} = -14.5$ kcal/mol in Table 5). The GGA exchange contributions to the barrier $E_x^{b(GGA)} = 18.1-18.7$ kcal/mol are substantially lower than $E_x^{b(KS)}$, and in fact close to the total KS exchange-correlation contribution $E_{xc}^{b(KS)} = 15.2$ kcal/mol (see Table 5). Therefore, in this case, as well as in the case a, $n/m = 1$, considered above, the GGA exchange functionals represent effectively both exchange and nondynamical correlation.

Still, the total GGA exchange-correlation contributions to the barrier, $E_{xc}^{b} = 7.2-9.8$ kcal/mol, are substantially lower than the KS E_{xc}^{b}, which leads to an equal underestimation of the barrier height E^b by the GGAs. (The total energies upon which the barrier energies in the GGA columns of Table 5 are based are KS/GGA energies, i.e., the only difference with the MRCI/KS energies is in the exchange-correlation terms, cf. eq 3.9.) The reason for this GGA error is the overestimation of the dynamical Coulomb correlation in the TS by the GGA correlation functionals.[17] These functionals which, supposedly, represent only the dynamical correlation produce a substantial negative contribution to the barrier $E_c^{b(GGA)}$ (see Table 5), while the dynamical correlation is expected to differ little between the TS and separated systems. As a remedy, it was proposed in ref 17 to modify the dependence of the approximate correlation functionals on the local polarization $\zeta(\mathbf{r}) = [\rho^{\uparrow}(\mathbf{r}) - \rho^{\downarrow}(\mathbf{r})]/\rho(\mathbf{r})$ in order to reduce the correlation for intermediate $|\zeta(\mathbf{r})|$ values between 0 and 1, which characterize the electron distribution in the H···H···H transition state. This modification will increase the barrier calculated for the $H + H_2$ reaction as well as for other radical abstraction reactions. Note that such a modification represents only a relatively minor change of current GGAs, since it neither changes the correlation functional for the closed-shell systems with $\zeta(\mathbf{r}) = 0$, nor does it change the functional for the separated H atom with $\zeta(\mathbf{r}) = 1$. Of course, it also does not influence the dominant exchange functional. With this relatively minor modification one can expect a good performance of GGAs for the considered case of the three-center three-electron bond.

(d) $n/m = 4/3$, Three-Center ($m = 3$) Four-Electron ($n = 4$) Bonds (Example: the TS of the S_N2 Reaction $F^- + CH_3F$). The reasoning given in the previous subsections helps also to interpret the GGA results for the S_N2 reaction $F^- + CH_3F$, which have been presented in section III. The TS of this reaction is characterized by a symmetrical three-center four-electron σ-bond F···C···F. The latter is represented with the nonbonding highest occupied molecular orbital (HOMO) ψ_0 which is, essentially, the in-phase combination of pσ orbitals of the F atoms, $\psi_0 \approx c_0[\sigma(F_A) + \sigma(F_B)]$, which is only very weakly σ-bonding within the fragment $[F_A\cdots F_B]^-$ due to the large distance, and the lowest occupied bonding MO ψ_+ which is actually the out-of-phase combination of σ orbitals of $[F_A\cdots F_B]^-$ stabilized by admixture of the p_σ orbital of the C atom, $\psi_+ \approx c_{1+}[\sigma(F_A) - \sigma(F_B)] - c_{2+}p_\sigma(C)$.

If the p_σ(C) were not involved, the ψ_+ and ψ_0 would describe two closed-shell F^- ions, like case b, and the exchange hole could localize completely on the F^- where the reference electron would be located. Complete localization is, however, prevented by the involvement of the p_σ(C). The GGA exchange energy, based on a fully localized model hole, therefore yields a too negative exchange energy. Although this error is very small percentagewise, its absolute magnitude is significant (of the 10 kcal/mol order of magnitude that is of interest here). If the nondynamical correlation would increase in the TS compared to the IC, the total hole would be more localized than the pure exchange hole, and we might wonder if the relatively localized GGA exchange hole does not again, as in the case $n/m = 1$ considered in the subsections a and c, cover exchange plus nondynamical correlation. However, the nondynamical correaltion is in this case not very different between IC and TS (there is only a small KS correlation contribution to the barrier $E_c^{b(KS)}$ in Table 2). This can be understood from the orbital picture. Indeed, population of both σ-bonding and σ-antibonding orbitals of $[F_A\cdots F_B]^-$ (i.e., of both ψ_0 and ψ_+) prevents an efficient nondynamical left−right correlation by the usual mechanism of double excitations from the bonding to the antibonding orbital.

Nondynamical correlation has to be produced by a strong configuration interaction of ψ_+ with the lowest unoccupied MO (LUMO) ψ_-, which correlates with the p_σ orbital of the C atom. However, this interaction is energetically unfavorable, since it leads to the excessive population of the less electronegative C atom. Thus, the abovementioned delocalization of the exchange hole, which is not countered with the localization effect of nondynamical correlation, is expected to produce a net delocalization of the total xc hole in the TS. The GGA exchange functionals with their background model of a localized hole are bound to build in nondynamical correlation in the TS, which in this case is spurious. Due to this spurious correlation in the exchange functional, the GGA functionals overestimate the relative stability of the TS of the S_N2 reaction as was shown in section III.

(e) $n/m = 3/2$, Two-Center ($m = 2$) Three-Electron ($n = 3$) Bonds (Examples: F_2^-, $(H_2O)_2^+$, Core Hole N_2^+). A two-center three-electron bond is formed by the p_σ orbitals in F_2^-, which can be considered a constituting fragment of the system $[F\cdots CH_3\cdots F]^-$. F_2^- is a stable radical anion with the equilibrium bond length $R_e(F-F) = 1.931$ Å[53] and dissociation energy $D_e = 30.2$ kcal/mol.[53,54] From a reasoning similar to that given in the previous subsection, one can suspect that GGAs overestimate the stability of F_2^-. Indeed, formation of F_2^- from F^- and F is accompanied by delocalization of the exchange hole over both F atoms. However, the nondynamical correlation in F_2^- is hampered by the unfavorable electron count, population of both bonding MO $\psi_+ = c_+[\sigma(F_A) + \sigma(F_B)]$ and antibonding (singly occupied) MO $\psi_- = c_-[\sigma(F_A) - \sigma(F_B)]$. In this situation one can suspect that the GGA exchange functionals might build in spurious correlation, thus overestimating the stability of F_2^-. Indeed, our self-consistent calculation of F_2^- with the BP functional yields the dissociation energy $D_e = 54.6$ kcal/mol, which is 24.4 kcal/mol higher than the cited reference value. The BLYP functional produces even larger dissociation energy $D_e = 62.0$ kcal/mol.

Another example of a two-center three-electron bond occurs in the hemibonded water dimer cation $[H_2O-H_2O]^+$ that has been considered in ref 8. It has been found that both BP and BLYP functionals overestimate the relative stability of this structure with respect to the proton transferred structure $OH-H_3O^+$. BP and BLYP predict that the hemibonded structure is more stable by 8.1 and 8.8 kcal/mol, respectively. Contrary to this, the reference CCSD(T) calculation indicates that the proton transferred structure is more stable than the hemibonded one by 7.7 kcal/mol. Extensive GGA calculations of dissociation energies of various dimer cations X_2^+ with two-center three-electron bonds have been performed in ref 7. It has been found

that GGAs systematically overestimate the dissociation energies, the corresponding errors range from 6 to 45 kcal/mol.

Yet another example, in fact the first, of the errors that arise in the two-orbital three-electron case has been the core hole ions that are generated by X-ray photoemission when a core electron is ionized in a symmetrical two-center system, like N_2. This case has been extensively analyzed by Noodleman et al.[55]

(f) $n/m = 1/2$, One-Electron ($n = 1$) Two-Center ($m = 2$) Bonds (H_2^+). Finally, we mention the famous extreme case, a one-electron molecular system, H_2^+. In this case the exact exchange represents just the self-interaction correction, and the exchange hole is obviously delocalized over both H atoms and the Coulomb correlation is absent. As has been shown in refs 6 and 8, GGAs greatly overestimate the energy of the dissociating H_2^+. Rather than going to the GGA energy of the H atom (and a proton at large distance), the GGA energy of H_2^+ at a distance of 5 Å proved to be ca. 50 kcal/mol too low.

From the point of view adopted in this paper, this trend can be interpreted as a gradual buildup of spurious nondynamical correlation at larger H−H separations which is erroneously produced by the GGA exchange functional. This functional corresponds implicitly to a localized hole, which can only be built up if the delocalized exchange hole is modified by the addition of a correlation hole that deepens the exchange hole around the reference electron at one H atom and cancels the exchange hole on the other H atom (cf. refs 45 and 47 for the two-electron H_2 molecule). This spurious correlation hole and the resulting "correlation energy" may alternatively be seen as an artificial overattractive self-interaction of the single electron.

To sum up, the examples given in subsections a−f justify the proposed qualitative rules. In standard bonding situations for closed-shell (subsections a and b) and open-shell (subsection c) molecular systems with "normal" electron counts, current GGAs or minor modifications (as required in case c**)** are expected to perform successfully. In this case the GGA exchange functionals represent efficiently both exchange and (if it takes place) molecular nondynamical correlation, while the GGA correlation functionals represent dynamical correlation. However, in the less standard bonding situations discussed in subsections d−f, GGAs are expected to overestimate the stability of molecular structures, for which the exchange hole is delocalized and unfavorable electron count hinders an efficient nondynamical correlation. In this case the GGA exchange functional builds in spurious excessive nondynamical correlation.

V. Conclusions

In this paper, the Kohn−Sham solution has been constructed from ab initio densities obtained with multireference configuration interaction (MRCI) calculations for the transition state (TS) and for the intermediate complex (IC) of the prototype symmetrical S_N2 reaction $F^- + CH_3F \rightarrow FCH_3 + F^-$. The corresponding KS exchange and correlation energies, E_x^{KS} and E_c^{KS}, have been used to analyze the performance of GGAs, which consistently underestimate the central barrier of the S_N2 reaction. The GGA exchange functionals have been found to be responsible for this error and, as a result, GGAs substantially underestimate the repulsive xc contribution to the barrier.

The overestimation of the exchange appears to be a typical feature of the GGA exchange functionals for molecules with covalent bonds. In this case the true KS exchange hole is delocalized over the interacting fragments, so that GGAs with their localized model holes are bound to overestimate the exchange energy. However, the localized model hole may be taken to represent both exchange and nondynamical correlation. In, for instance, the prototype case of N_2 the GGA correlation functionals lack the nondynamical correlation and the exchange "error" actually brings in this nondynamical correlation energy, thus helping the GGA functionals to reproduce very well the total Kohn−Sham xc energies. The difference between the case of N_2, which is fortunate for the GGAs, and the unfortunate case of the S_N2 reaction lies in nondynamical correlation. The GGA exchange functionals, which could better be called exchange-nondynamical correlation functionals, will always yield significant nondynamical (left−right) correlation, and are erroneous when there is in reality little such correlation. A qualitative rule has been put forward to distinguish types of bonding with strong nondynamical correlation from those with a relatively weak correlation.

With this rule one can attempt to predict the performance of GGAs for various types of bonding. For systems with two-center two-electron bonds (standard covalent bonds) and two-center four-electron Pauli repulsion (interacting closed shells) current GGAs are expected to perform successfully, as they would, with relatively minor modification, for three-center three-electron bonds. In these cases the GGA exchange functional represents exchange and (if it takes place) nondynamical Coulomb correlation, while the GGA correlation functional represents dynamical Coulomb correlation. Contrary to this, for systems with three-center four-electron bonds (the TS of the S_N2 reaction), two-center three-electron bonds, and two-center one-electron bonds, for which the exchange hole is delocalized over all interacting fragments and efficient nondynamical correlation is hampered by the unfavorable electron count, the exchange GGAs are expected to build up spurious excessive nondynamical correlation, thus overestimating the relative stability of these systems.

The results of the present and cited papers stress the importance of further development of approximate DFT methods in order to improve their performance in the abovementioned problematic cases. In this respect, obvious candidates are the hybrid DFT/HF functionals, such as BHLYP[56] and B3LYP,[57] in which the GGA exchange functionals based on localized model holes are mixed with the Hartree−Fock exchange functional, which can represent a delocalized hole. Arguably, such an admixture represents a rather major change from the original GGAs. As has been shown in ref 20, B3LYP yields the improved barrier height 9.43 kcal/mol for the S_N2 reaction 1.1, so that the error is reduced to −4 kcal/mol. For the analogous reaction $Cl^- + CH_3Cl$ B3LYP produces a similar error of −4.5 kcal/mol.[20,37] While these errors are still appreciable by chemical standards, one can hope for improvement due to further refinement of hybrid functionals. Still, the hybrid DFT/HF approach has its own limitations. For example, in order to produce the exact self-interaction correction in the case of H_2^+, a hybrid functional should contain 100% of HF exchange. On the other hand, the H_2 molecule is an example of the extreme opposite; the exact exchange contribution has to go to zero in the dissociation limit.[8,58] Clearly, such opposite requirements cannot be satisfied with a DFT/HF hybrid functional with fixed mixing coefficients (the only type currently available). An alternative, more natural refinement of GGAs could be, in principle, achieved by the inclusion of functionals of higher order derivatives (Laplacians)[16] or of the kinetic energy density τ of the KS orbitals ("meta-GGAs"[59−62])

$$\tau(\mathbf{r}) = {}^1/_2 \sum_{i=1}^{N} |\nabla \psi_i(\mathbf{r})|^2 \qquad (5.1)$$

Interestingly enough, the function τ can distinguish between a situation a with a normal bond as in N_2 or F_2 and situations d and e where the related antibonding orbital is occupied. Let us compare, for example, F_2 and F_2^- and consider the behavior of $\tau(\mathbf{r})$ around the bond midpoint $\mathbf{r}_m$, at which the density gradient is zero $\nabla\rho(\mathbf{r}_m) = 0$. For F_2 only the σ-bonding orbital ψ_+ is occupied and, because of the form of this orbital, $\tau(\mathbf{r}_m)$ is also zero.[63] Contrary to this, as was mentioned in subsection e, in the case of F_2^- the antibonding orbital ψ_- is also occupied, but the gradient of this orbital is nonzero at $\mathbf{r}_m$,[63] thus producing a positive value of $\tau(\mathbf{r}_m)$. Using this feature of the function τ, one can attempt to correct GGAs in the bond midpoint region. The current GGAs are reduced to the LDA in the bond midpoint region (cf. Figure 3) because of the vanishing GGA gradient argument $x(\mathbf{r}) = |\nabla\rho(\mathbf{r})|/\rho^{4/3}(\mathbf{r})$.

Acknowledgment. We gratefully acknowledge support for B.E. from the Netherlands Organization for Scientific Research (NWO) through the Priority Programme for Materials Science, section Computational Materials Science (PPM-CMS).

References and Notes

(1) Kohn, W.; Becke, A. D.; Parr, R. G. *J. Phys. Chem.* **1996**, *100*, 12974.
(2) Perdew, J. P. *Phys. Rev. B* **1986**, *33*, 8822 (Erratum: *Phys. Rev. B* **1986**, *34*, 7406).
(3) Lee, C.; Yang, W.; Parr, R. G. *Phys. Rev. B* **1988**, *37*, 785.
(4) Becke, A. *Phys. Rev. A* **1988**, *38*, 3098.
(5) Perdew, J. P.; Burke, K.; Wang, Y. *Phys. Rev. B* **1996**, *54*, 16533.
(6) Bally, T.; Sastry, G. N. *J. Phys. Chem. A* **1997**, *101*, 7923.
(7) Braida, B.; Hiberty, P. C.; Savin, A. *J. Phys. Chem. A* **1998**, *102*, 7872.
(8) Sodupe, M.; Bertran, J.; Rodriguez-Santiago, L.; Baerends, E. J. *J. Phys. Chem. A* **1998**, *103*, 166.
(9) Johnson, B. G.; Gonzales, C. A.; Gill, P. M. W.; Pople, J. A. *Chem. Phys. Lett.* **1994**, *221*, 100.
(10) Baker, J.; Muir, M.; Andzelm, J. *J. Chem. Phys.* **1995**, *102*, 2063.
(11) Porezag, D.; Pederson, M. R. *J. Chem. Phys.* **1995**, *102*, 9345.
(12) Jursic, B. S. *Theor. Comput. Chem.* **1996**, *4*, 709.
(13) Skokov, S.; Wheeler, R. A. *Chem. Phys. Lett.* **1997**, *271*, 251.
(14) Chermette, H.; Razafinjanahary, H.; Carrion, L. *J. Chem. Phys.* **1997**, *107*, 10643.
(15) Csonka, G. I.; Johnson, B. G. *Theor. Chem. Acc.* **1998**, *99*, 158.
(16) Filatov, M.; Thiel, W. *Chem. Phys. Lett.* **1998**, *295*, 467.
(17) Schipper, P. R. T.; Gritsenko, O. V.; Baerends, E. J. *J. Chem. Phys.* **1999**, *111*, 4056.
(18) Deng, L.; Branchadell, V.; Ziegler, T. *J. Am. Chem. Soc.* **1994**, *116*, 10645.
(19) Glukhovtsev, M. N.; Bach, R. D.; Pross, A.; Radom, L. *Chem. Phys. Lett.* **1996**, *260*, 558.
(20) Streitwieser, A.; Choy, G. S.-C.; Abu-Hasanayn, F. *J. Am. Chem. Soc.* **1997**, *119*, 5013.
(21) Almbladh, C. O.; Pedroza, A. C. *Phys. Rev. A* **1984**, *29*, 2322.
(22) Aryasetiawan, F.; Stott, M. J. *Phys. Rev. B* **1986**, *34*, 4401.
(23) Zhao, Q.; Morrison, R. C.; Parr, R. G. *Phys. Rev. A* **1994**, *50*, 2138.
(24) Morrison, R. C.; Zhao, Q. *Phys. Rev. A* **1995**, *51*, 1980.
(25) Buijse, M. A.; Baerends, E. J.; Snijders, J. G. *Phys. Rev. A* **1989**, *40*, 4190.
(26) Gritsenko, O. V.; van Leeuwen, R.; Baerends, E. J. *Phys. Rev. A* **1995**, *52*, 1870.
(27) Gritsenko, O. V.; van Leeuwen, R.; Baerends, E. J. *J. Chem. Phys.* **1996**, *104*, 8535.
(28) Gritsenko, O. V.; Schipper, P. R. T.; Baerends, E. J. *J. Chem. Phys.* **1997**, *107*, 5007.
(29) Schipper, P. R. T.; Gritsenko, O. V.; Baerends, E. J. *Phys. Rev. A* **1998**, *A57*, 1729.
(30) Schipper, P. R. T.; Gritsenko, O. V.; Baerrends, E. J. *Theor. Chem. Acc.* **1998**, *99*, 329.
(31) Ingamells, V. E.; Handy, N. C. *Chem. Phys. Lett.* **1996**, *248*, 373.
(32) Tozer, D. J.; Ingamells, V. E.; Handy, N. C. *J. Chem. Phys.* **1996**, *105*, 9200.
(33) Pellerite, M. J.; Brauman, J. I. *J. Am. Chem. Soc.* **1983**, *105*, 2672.
(34) Larson, J. W.; McMahon, T. B. *J. Am. Chem. Soc.* **1985**, *107*, 766.
(35) Cyr, D. M.; Scarton, M. G.; Johnson, M. A. *J. Chem. Phys.* **1993**, *99*, 4869.
(36) Wladkowski, B. D.; Allen, W. D.; Brauman, J. I. *J. Phys. Chem.* **1994**, *98*, 13532.
(37) Glukhovtsev, M. N.; Pross, A.; Radom, L. *J. Am. Chem. Soc.* **1995**, *117*, 2024.
(38) Saunders: V. R.; van Lenthe, J. H. *Mol. Phys.* **1983**, *48*, 923.
(39) Dunning, T. H. *J. Chem. Phys.* **1971**, *55*, 716.
(40) Dunning, T. H. *J. Chem. Phys.* **1989**, *90*, 1007.
(41) Vetter, R.; Zülicke, L. *J. Am. Chem. Soc.* **1990**, *112*, 5136.
(42) Szabo, A.; Ostlund, N. S. *Modern Quantum Chemistry*; McGraw-Hill: New York, 1989; Vol. 2.
(43) Schipper, P. R. T.; Gritsenko, O. V.; Baerends, E. J. *Theor. Chem. Acc.* **1997**, *98*, 16.
(44) Luken, W. L. *Int. J. Quantum Chem.* **1982**, *22*, 889.
(45) Buijse, M. A.; Baerends, E. J. Fermi holes and Coulomb holes. In *Electronic Density Functional Theory of Molecules, Clusters and Solids*; Ellis, D. E., Ed.; Kluwer Academic Publishers: Dordrecht, 1995; p 1.
(46) Süle, P.; Gritsenko, O. V.; Nagy, A.; Baerends, E. J. *J. Chem. Phys.* **1995**, *103*, 10085.
(47) Baerends, E. J.; Gritsenko, O. V. *J. Phys. Chem.* **1997**, *101*, 5383.
(48) Buijse, M. A. Electron Correlation. Fermi and Coulomb holes, dynamical and nondynamical correlation. Ph.D. Thesis, Vrije Universiteit, 1991.
(49) Perdew, J. P. Unified Theory of Exchange and Correlation beyond the Local Density Approximation. In *Electronic Structure of Solids*; Ziesche, P., Eschrig, H., Eds.; Akademie Verlag: Berlin, 1991; p 11.
(50) Perdew, J. P.; Chevary, J. A.; Vosko, S. H.; Jackson, K. A.; Pederson, M. R.; Singh, D. J.; Fiolhais, C. *Phys. Rev. B* **1992**, *46*, 6671.
(51) Lie, G. C.; Clementi, E. *J. Chem. Phys.* **1974**, *60*, 1275.
(52) Gritsenko, O. V.; Schipper, P. R. T.; Baerends, E. J. *Phys. Rev. A* **1998**, *57*, 3450.
(53) Hiberty, P. C.; Humbel, S.; Archirel, P. *J. Phys. Chem.* **1994**, *98*, 11697.
(54) Huber, K. P.; Herzberg, G. *Constants of Diatomic Molecules*; Van Nostrand-Reinhold: New York, 1979.
(55) Noodleman, L.; Post, D.; Baerends, E. J. *Chem. Phys.* **1982**, *64*, 159.
(56) Becke, A. D. *J. Chem. Phys.* **1993**, *98*, 1372.
(57) Becke, A. D. *J. Chem. Phys.* **1993**, *98*, 5648.
(58) Gritsenko, O. V.; van Leeuwen, R.; Baerends, E. J. *Int. J. Quantum Chem.* **1996**, *60*, *1375*.
(59) Proynov, E. I.; Ruiz, E.; Vela, A.; Salahub, D. R. *Int. J. Quantum Chem.* **1995**, *29*, 61.
(60) Becke, A. D. *J. Chem. Phys.* **1996**, *104*, 1040.
(61) van Voorhis, T.; Scuseria, G. E. *J. Chem. Phys.* **1998**, *109*, 400.
(62) Perdew, J. P.; Kurth, S.; Zupan, A.; Blaha, P. *Phys. Rev. Lett.* **1999**, *82*, 2544.
(63) Gritsenko, O. V.; Baerends, E. J. *Theor. Chem. Acc.* **1997**, *96*, 44.